Available online at www.sciencedirect.com
ScienceDirect
Polymer 49 (2008) 1305–1311
polymer
www.elsevier.com/locate/polymer

Studies on thermal properties of PS nanocomposites for the effect of intercalated agent with side groups

Huei-Kuan Fu [a], Chih-Feng Huang [a], Jieh-Ming Huang [b], Feng-Chih Chang [a,*]

[a] *Institute of Applied Chemistry, National Chiao-Tung University, Hsin-Chu, Taiwan*
[b] *Department of Chemical Engineering, Van Nung University, Chung-Li 32054, Taiwan*

Received 31 August 2007; received in revised form 3 January 2008; accepted 9 January 2008
Available online 12 January 2008

Abstract

Polystyrene-layered silicate nanocomposites were prepared from three new organically modified clays by emulsion polymerization method. These nanocomposites were exfoliated up to 3 wt% content of pristine clay relative to the amount of polystyrene (PS). The intercalated agents C_{20}, C_{20}–4VB, and C_{20}–POSS intercalated into the galleries result in improved compatibility between hydrophobic polymer and hydrophilic clay and facilitate the well dispersion of exfoliated clay in the polymer matrix. Results from X-ray diffraction, TEM and Fourier transform infrared spectroscopy indicate that these intercalated agents are indeed intercalated into the clay galleries successfully and these clay platelets are exfoliated in resultant nanocomposites. Thermal analyses of polystyrene-layered silicate nanocomposites compared with virgin PS indicate that the onset degradation temperature ca. 25 °C increased and the maximum reduction in coefficient of thermal expansion (CTE) is ca. 40% for the C_{20}–POSS/clay nanocomposite. In addition, the glass transition temperatures of all these nanocomposites are higher than the virgin PS.

Keywords: Nanocomposites; Polystyrene; POSS

1. Introduction

Polystyrene (PS) is one of the most mass-productive and commercialized polymers. Recently, polystyrene (PS)/clay nanocomposites have been reported by several researchers [1–6]. Over the last decade, the use of organically modified montmorillonite as an additive has been intensively studied because of its improved thermal [7–10] and mechanical properties [11–16]. The most promising composite systems would be the hybrids based on organic polymers and inorganic clay minerals consisting of silicate layers [1,11,15,17–27]. Polymer–clay nanocomposites were first synthesized by a Toyota research group [18,19]. They reported that individual layers (about 1 nm thickness) of clay particles are completely exfoliated in a continuous polymer matrix as revealed by X-ray diffraction (XRD) and transmission electron microscopy (TEM). The incorporation of organophilic clays, commonly montmorillonites (MMT), into polymers dramatically enhances its barrier, thermal and mechanical properties, since such nanofillers display a large surface for interactions with polymer matrix. During the past few years, great attention has been paid on silsesquioxane based nanocomposite. The POSS moiety is expected to act as a nano-scale filler to modify polymer matrix and results in nanocomposites with improved mechanical and thermal properties [28–30].

The chemical structure of montmorillonite consists of two fused silica tetrahedral sheets sandwiching an edge-shared octahedral sheet of either magnesium or aluminum hydroxide. The clay can be functionalized by various organic cations through ion exchange where the metal ions are replaced by organic cations intercalated into the silicate layers. Its hydrophilic nature and ionic exchange capacity allow the silicate mineral to be intercalated by organic cations such as alkylammonium, to make the clay organophilic and compatible with polymers [31,32]. High homogeneity for the dispersion of

* Corresponding author. Tel./fax: +886 3 5131512.
E-mail address: changfc@mail.nctu.edu.tw (F.-C. Chang).

0032-3861/$ - see front matter © 2008 Elsevier Ltd. All rights reserved.
doi:10.1016/j.polymer.2008.01.013

clays in the matrix usually requires the intercalated agents to be highly compatible with silicate clay and polymer matrix.

Several ways to make polymer-layered silicate nanocomposites have been demonstrated, including solution mixing, melt blending, and in situ polymerization [33–35]. In general, polymer-layered silicate nanocomposites can be divided into two categories. The intercalated polymer-layered silicate nanocomposites have layered clay dispersed in a polymer matrix with polymer chains inserted into clays layers but retain their lateral order. The exfoliated ones consist of fully delaminated clay platelets dispersed individually in polymer matrix. In general, the exfoliated structure is more effective in improving the properties of the polymer.

In this study, three PS nanocomposites were prepared by emulsion polymerization using C_{20}, C_{20}–4VB, and C_{20}–POSS-treated clays as shown in Scheme 1. The type of the nanocomposites produced was elucidated using X-ray diffraction and transmission electron microscopy. IR spectroscopic analysis confirmed the existence of the intercalated agents in the clay galleries. Properties of these polymer–clay nanocomposites were characterized by thermogravimetric analysis, differential scanning calorimeter, gel permeation chromatography, coefficient of thermal expansion, and mechanical properties.

2. Experimental

2.1. Materials

Sodium montmorillonite (Na^+–MMT) with 1.45 mequiv/g cationic exchange capacity (CEC) was purchased from Nanocor Co. Most chemicals used in this study, including monomeric styrene, chemically pure acetone, methanol, tetrahydrofuran, acetonitrile, potassium hydroxide (KOH), triethylamine, and trichloro [4-(chloromethyl)phenyl] silane were acquired from the Aldrich Chemical Co., Inc. The styrene monomer was purified by removing the inhibitor with the aid of an inhibitor-removal column. Sodium dodecyl sulfate (SDS) and hydrochloric acid were both obtained from Curtin Matheson Scientific, Inc. Potassium persulfate ($K_2S_2O_8$) and aluminum sulfate [$Al_2(SO_4)_3$] were acquired from Fisher Scientific Co., USA. *N*,*N*-Dimethyloctadecylamine (C_{20}) and 4-vinylbenzyl chloride (4VB) were obtained from Acros Organics, USA. Trisilanolisobutyl polyhedral oligomeric silsesquioxane (POSS) was obtained from Hybrid Plastics, Inc.

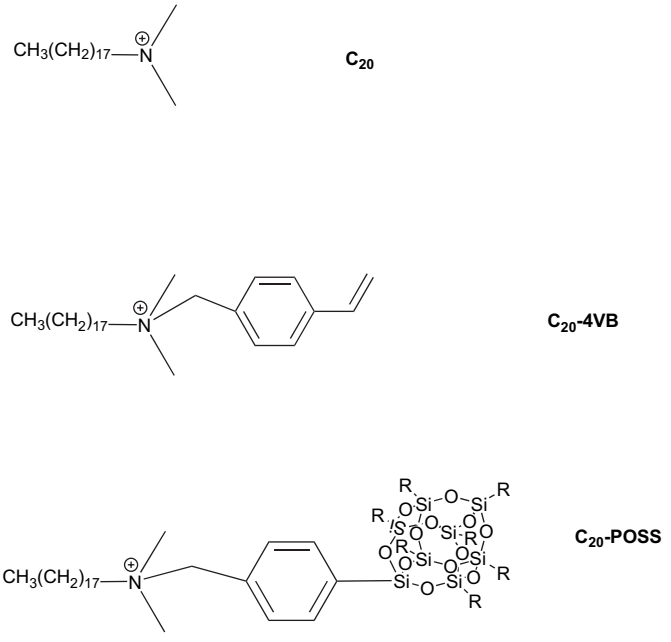

Scheme 1. Intercalation agents for organic modified clays preparation.

2.2. Preparation of POSS–Cl compound

The corner-capping reaction was employed to prepare POSS–Cl compound as shown in Scheme 2. Trisilanolisobutyl polyhedral oligomeric silsesquioxane (**1**, 3 g) and Et_3N (1.26 g) were added into a 100 mL two-neck round bottom flask and stirred continuously for 3 h under nitrogen, then 20 mL THF was added into the flask at 0 °C for 1 h. After stirring at 0 °C under nitrogen, triethylamine and trichloro[4-(chloromethyl)phenyl]silane (**2**, 1.28 g) in THF (10 mL) were added dropwise into the solution and stirred at 0 °C. The cooling bath was removed and the solution was stirred continuously for additional 7.5 h under nitrogen. The POSS type compound and $HNEt_3$–Cl byproduct were separated by filtration. The clear THF solution was dropped into a beaker of acetonitrile and rapidly stirred. The resulting product (**3**) was collected and dried in a vacuum oven for 24 h. ^{1}H NMR ($CDCl_3$) δ: 7.59 (d, 2H), 7.33 (d, 2H), 4.52 (s, 2H), 1.92–1.62 (m, 7H), 1.09–0.85 (m, 42H), 0.75–0.48 (m, 14H).

2.3. Preparation of C_{20}–4VB intercalated agent

The intercalated agent of C_{20}–4VB was prepared according to the pathway shown in Scheme 3a. *N*,*N*-Dimethyloctadecylamine (C_{20}, 4.2 mL) and 4-vinylbenzyl chloride (4VB, 1.87 g) in acetone (10 mL) were refluxed at 60 °C under nitrogen for 5 h. After cooling, the mixture was washed with cold acetone and the volatiles were removed in vacuum oven for 24 h at 65 °C. ^{1}H NMR ($CDCl_3$) δ: 7.56 (d, 2H), 7.38 (d, 2H), 6.65 (q, 1H), 5.75 (d, 1H), 5.31 (d, 1H), 4.96 (s, 2H), 3.39 (t, 2H), 3.23 (s, 6H), 1.72 (m, 2H), 1.23 (m, 30H), 0.82 (t, 3H).

2.4. Preparation of C_{20}–POSS intercalated agent

The intercalated agent of C_{20}–POSS was prepared according to the pathway shown in Scheme 3b. *N*,*N*-Dimethyloctadecylamine (C_{20}, 1.49 g) and POSS–Cl compound (5.68 g) in acetone (15 mL) were refluxed at 60 °C under nitrogen for 24 h. After cooling, the mixture was evaporated by a rotatory evaporator and then Et_2O (20 mL) was added. The solution was extracted with deionized water three times (150 mL × 3). The organic phase was dried with $MgSO_4$ and evaporated by a rotatory evaporator to obtain the C_{20}–POSS intercalated agent. ^{1}H NMR ($CDCl_3$) δ: 7.68 (d, 2H), 7.58 (d, 2H), 5.03 (s,

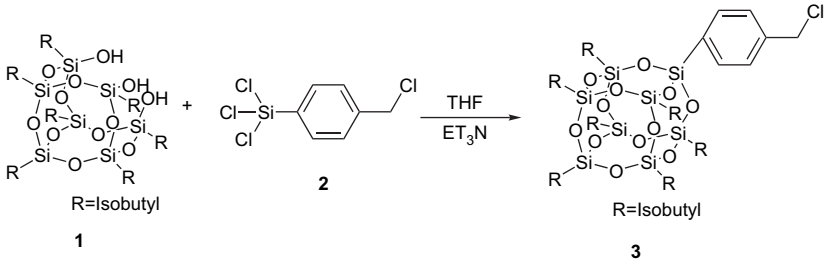

Scheme 2. Synthesis of POSS–Cl compound.

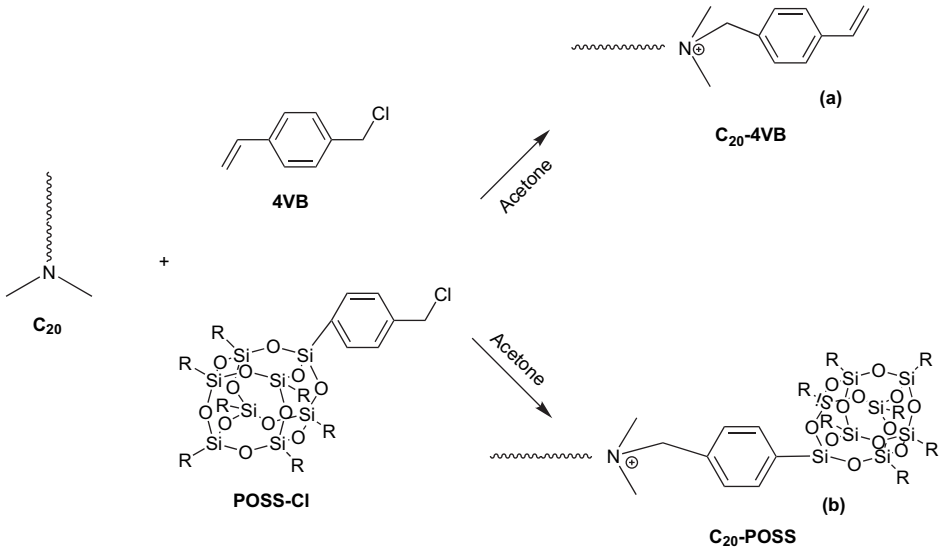

Scheme 3. Synthesis of the C_{20}–4VB and C_{20}–POSS intercalated agents.

2H), 3.42 (t, 2H), 3.30 (s, 6H), 1.81 (m, 7H), 1.41 (m, 2H), 1.26 (m, 30H), 0.90 (m, 42H), 0.82 (t, 3H), 0.59 (m, 14H).

2.5. Preparation of C_{20}-, C_{20}–4VB-, and C_{20}–POSS-modified clays

Na^+–MMT (0.3 g) was dispersed in 1 L deionized water at 80 °C and stirred continuously for 4 h. C_{20} (0.18 g), C_{20}–4VB (0.22 g) or C_{20}–POSS (0.63 g) in water (5 mL) was placed into another flask, 10% hydrochloric acid (1 mL) and ethanol (5 mL) were added and then stirred at 80 °C for 1 h. This intercalating agent solution was then poured into the clay suspension solution and stirred vigorously at 80 °C for 4 h. The white precipitate was filtered to remove water and washed thoroughly with warm water until no chloride could be detected by aqueous $AgNO_3$ solution, and then dried overnight in a vacuum oven at room temperature.

2.6. Preparation of polystyrene/clay nanocomposites

Desired amounts of organic modified clay, KOH, SDS and styrene monomer were added in a two-neck round bottom flask equipped with a stirring bar. The mixture was heated to 80 °C and stirred under N_2, desired quantity of $K_2S_2O_8$ was added slowly to the mixture. Polymerization was carried out at 80 °C for 8 h and then cooled to room temperature. Aqueous aluminum sulfate (2.5%, 10 mL) was added into the polymerized emulsion, followed by adding dilute hydrochloric acid (10 mL) with stirring. Finally, acetone was added to break down the emulsion completely, and the polymer product was washed several times with methanol and distilled water and then dried in a vacuum oven at 80 °C for 24 h. Similar procedures were employed to prepare virgin polystyrene.

2.7. Instrumentations

Wide-angle X-ray diffraction (WAXD) spectrum was recorded on powdered sample using a Rigaku D/max-2500 type X-ray diffraction instrument. The radiation source used was Ni-filtered, Cu Kα radiation ($\lambda = 1.54$ Å). The sample was mounted on a circular sample holder, the scanning rate was 0.6°/min from $2\theta = 1$–20. A Hitachi H-7500 transmission electron microscopy (100 kV) was used to examine clay morphology and orientation. The sample was ultramicrotomed at room temperature using a diamond knife using a Leica Ultracut UCT Microtome to give 70 nm thick sections. Thermogravimetric analysis (TGA) was performed on a TA Instruments Q50 apparatus. The sample (5–10 mg) was placed in a Pt cell at a scan rate of 20 °C/min from 30 to 800 °C under nitrogen. The calorimetric measurement was performed use a TA Instruments Differential Scanning Calorimeter (DSC-2010)

to measure the glass transition temperature (T_g). The sample was preheated at a scan rate of 20 °C/min from 30 to 150 °C. In DSC measurement of the sample was cooled to 10 °C quickly from the melt of the first scan and the second scan rate was 20 °C/min from 30 to 150 °C. The T_g value was taken as the midpoint of the heat capacity transition between the upper and lower points of deviation from the extrapolated liquid and glass lines. Molecular weights and molecular weight distributions were determined by gel permeation chromatography (GPC) using a Waters 510 HPLC equipped with a 410 Differential Refractometer, a refractive index (UV) detector, and three Ultrastyragel columns (100, 500, and 10^3 Å) connected in series in the order of increasing pore size. The molecular weight calibration curve was obtained using polystyrene standards. ^{1}H NMR spectroscopic analyses were performed using a Varian Uniytinova-500 NMR Spectrometer at 500 MHz. All spectra were recorded using $CDCl_3$ as the solvent and TMS as the external standard. Coefficient of thermal expansion was obtained using a TA 2940 Thermomechanical Analyzer (TMA). The force applied was 0.005 N and it was heated at a rate of 5 °C/min from 25 to 150 °C.

3. Results and discussion

Structures of intercalated agents used to modify the clays are shown in Scheme 1.

3.1. Characterizations of C_{20}-, C_{20}–4VB-, and C_{20}–POSS-modified clays

Fig. 1 shows the XRD curves for the starting and modified clays. The *d* spacing indicates the interlayer spacing of the silicate layers calculated from the peak position using the Bragg equation. The original clay with an intergallery spacing of 1.28 nm ($2\theta = 6.92°$) increases to 3.95 nm for C_{20} ($2\theta = 2.23°$), 3.33 nm for C_{20}–4VB ($2\theta = 2.66°$), and 3.80 nm for C_{20}–POSS ($2\theta = 2.33°$). The results indicate that these intercalated agents are successfully intercalated into the gallery and results are summarized in Table 1. When the C_{20}–POSS is inserted between the galleries of the clay, the *d* spacing is increased from 1.28 nm for original clay to 3.80 nm, implying that the C_{20}–POSS is inserted inside the gallery of the silicate.

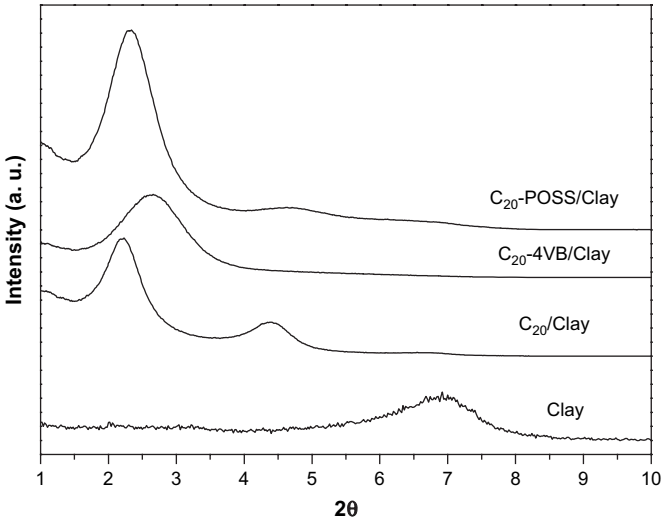

Fig. 1. X-ray diffraction patterns of pure clay and intercalated clays.

Table 1
Basal spacing and organic fraction of the OMMT

Sample	(001) Basal spacing (nm)	Organic fraction[a] (%)
Clay	1.28	–
C_{20}/clay	4.2	53.3
C_{20}–4VB/clay	3.53	47.3
C_{20}–POSS/clay	3.92	37.5

[a] Organic fraction was based on TG analyses.

3.2. Characterizations of polystyrene/clay nanocomposites

Fig. 2 shows X-ray diffraction patterns of C_{20}/clay/PS, C_{20}–4VB/clay/PS and C_{20}–POSS/clay/PS nanocomposites. Essentially no peak can be detected for all nanocomposites from C_{20}-, C_{20}–4VB-, and C_{20}–POSS-modified clays, implying that they all have exfoliated structure. XRD alone may lead to false result in terms of the extent of exfoliation. As a result, TEM observations are necessary to further verify the extent of delamination and exfoliation. Either intercalated or exfoliated nanocomposite can be distinguished on the basis of transmission electron microscopy (TEM). TEM images of C_{20}/clay/PS, C_{20}–4VB/clay/PS and C_{20}–POSS/clay/PS are shown in Fig. 3. In Fig. 3b, C_{20}–4VB/clay/PS shows full dispersion and exfoliation of the clay platelets within the PS matrix because the intercalated agent of C_{20}–4VB containing a vinylbenzyl group allows for styrene polymerization taking

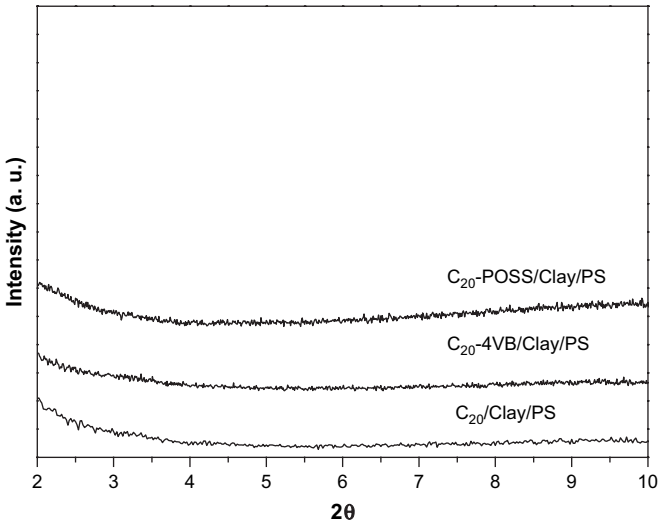

Fig. 2. XRD spectra of the three surfactant-containing nanocomposites indicating the extent of delamination.

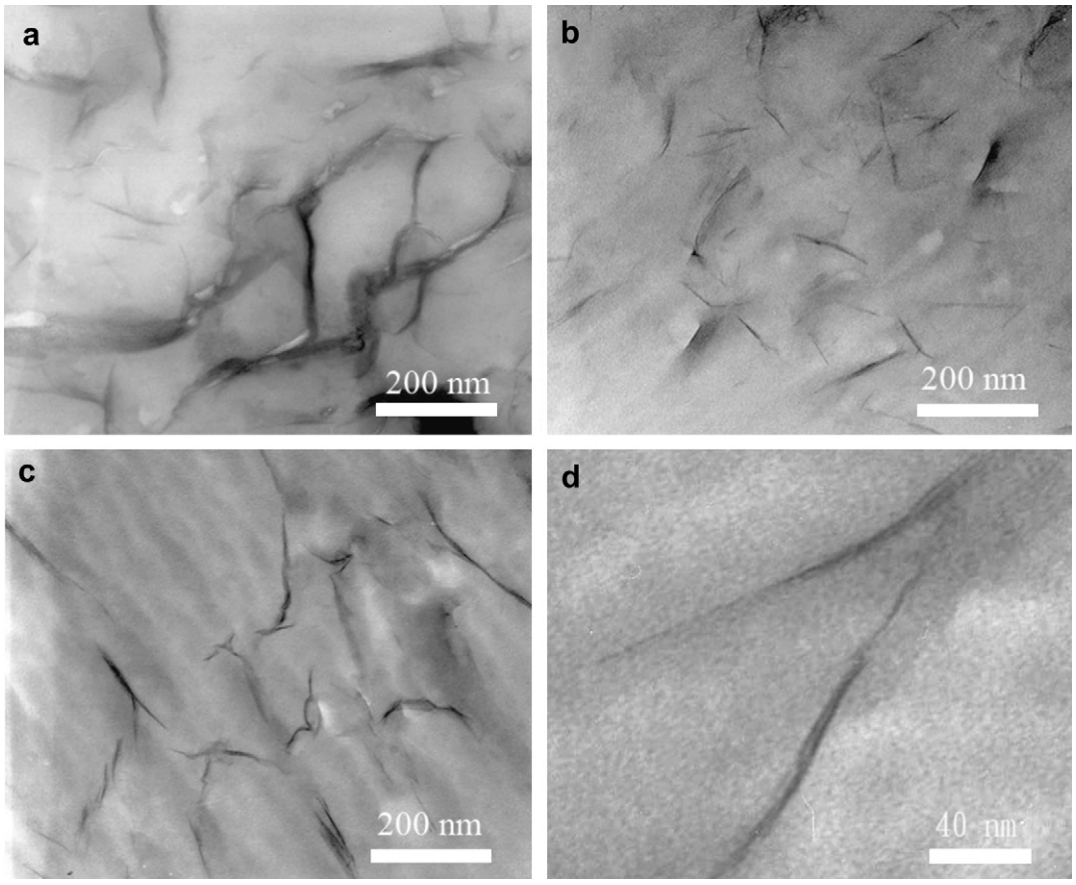

Fig. 3. TEM images of (a) C_{20}, (b) C_{20}–4VB, (c) C_{20}–POSS (low magnification), and (d) C_{20}–POSS (high magnification)-treated nanocomposites.

place within the clay gallery. In Fig. 3a, these clay platelets of the C_{20}/clay modified nanocomposite are mainly exfoliated, but in some regions they are aggregated and intercalated. In Fig. 3c, the image shows mainly the exfoliated structures for the C_{20}–POSS-modified nanocomposite.

3.3. Glass transition temperatures

Fig. 4 and Table 2 show that the pure PS exhibits a heat flow change at approximately 100 °C, corresponding to the T_g of PS. All DSC thermograms display single glass transition temperature in the experimental temperature range. C_{20}/clay, C_{20}–4VB/clay, and C_{20}–POSS/clay-modified nanocomposites all show slightly higher T_g compared to the pure PS.

3.4. Molecular weights of the nanocomposites

Table 3 shows the molecular weight and polydispersities of the PS and PS/silicate nanocomposites through emulsion polymerization. The sample for the molecular weight determination was filtered to remove all clay content before measurement and the results are shown in Table 3. From the table, M_n (or M_w) of the PS in PS/clay nanocomposites is higher, suggesting that clay may either act as a catalytic agent, resulting in a higher molecular weight of the PS with proceeding polymerization.

3.5. TG analyses

Figs. 5 and 6 present the thermal stabilities of the C_{20}-, C_{20}–4VB-, and C_{20}–POSS-modified clays and the corresponding nanocomposites measured under nitrogen gas. Generally, the incorporation of clay into the polymer matrix is able to enhance thermal stability by acting as a superior insulator

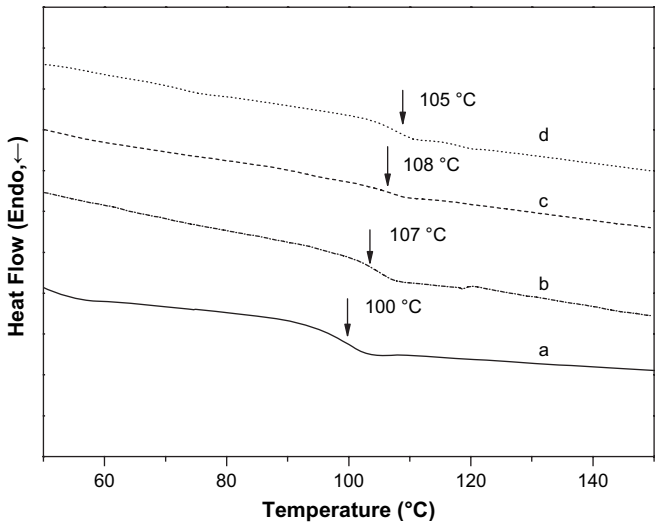

Fig. 4. DSC curves glass transition temperature of (a) PS, (b) the nanocomposites formed used C_{20}, (c) the nanocomposites formed used C_{20}–4VB, and (d) the nanocomposites formed used C_{20}–POSS.

Table 2
Results of thermal and mechanical properties of polystyrene and polystyrene nanocomposites

Sample	T_g[a] (°C)	$T_{0.05}$[b] (°C)	$T_{0.5}$[c] (°C)	Char at 600 °C[d] (%)	CTE (μm/m °C)
PS	100	390	424	0	164
C_{20}/clay/PS	107	405		1.59/1.4	120
C_{20}–4VB/clay/PS	108	402	454	1.59/1.59	134
C_{20}–POSS/clay/PS	105	415	457	1.98/2.4	100

[a] Glass transition temperature (T_g).
[b] 5% Degradation temperature ($T_{0.05}$).
[c] 50% Degradation temperature ($T_{0.5}$).
[d] Char at 600 (°C)% (expected %/experiment %).

Table 3
Molecular weights of polystyrene and polystyrene nanocomposites

Sample	M_n[a] ($\times 10^4$)	M_w[b] ($\times 10^4$)	PDI[c] (M_w/M_n)
PS	34.5	53.1	1.54
C_{20}/clay/PS	47.5	58.6	1.23
C_{20}–4VB/clay/PS	45.2	57.4	1.27
C_{20}–POSS/clay/PS	47.7	58.7	1.23

[a] Number-average molecular weights (M_n).
[b] Weight-average molecular weights (M_w) were determined by GPC.
[c] Polydispersity index, M_w/M_n.

and mass transport barrier to the volatile products generated during decomposition. Fig. 5 shows TGA traces for these intercalated clays. The C_{20}–POSS/clay decomposes at a higher temperature of 262 °C while C_{20}/clay and C_{20}–4VB/clay decompose at 189 and 243 °C, indicating that the C_{20}–POSS is thermally more stable than the C_{20} and C_{20}–4VB. Thereby, the clay intercalated with C_{20}–POSS has better thermal stability relative to those intercalated with C_{20} and C_{20}–4VB.

All surfactant-modified nanocomposites show better thermal stability than the virgin PS as shown in Fig. 6. The decomposition temperatures for 5% weight loss of C_{20}-, C_{20}–4VB-, and C_{20}–POSS-modified nanocomposites are 15, 12, and 25 °C higher than the virgin PS. This observed enhancement

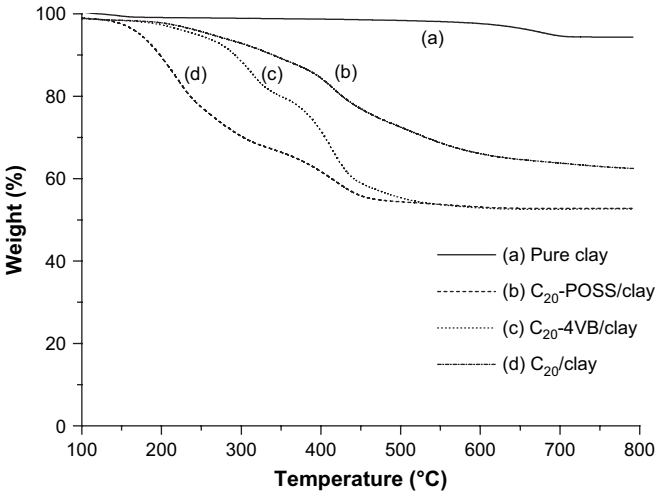

Fig. 5. TGA curves of (a) pure clay, (b) C_{20}–POSS/clay, (c) C_{20}–4VB/clay, and (d) C_{20}/clay.

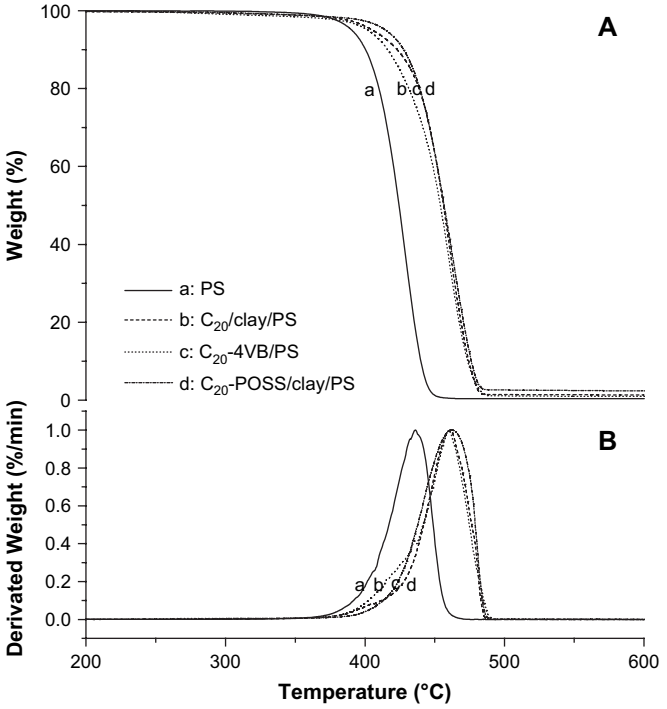

Fig. 6. (A) TGA and (B) DTG curves of the nanocomposites under a nitrogen atmosphere: (a) pure PS, (b) the nanocomposite formed with C_{20}, (c) the nanocomposite formed with C_{20}–4VB, and (d) the nanocomposite formed with C_{20}–POSS.

in the thermal properties is due to the presence of the clay to act as barriers to minimize the permeability of volatile degradation products out from the material. The values of 5 and 50% weight loss temperatures and the corresponding char yields are summarized in Table 1.

3.6. Coefficient of thermal expansion

Dimensional stability is critical in many applications, poor dimensional stability can cause warping or other changes in

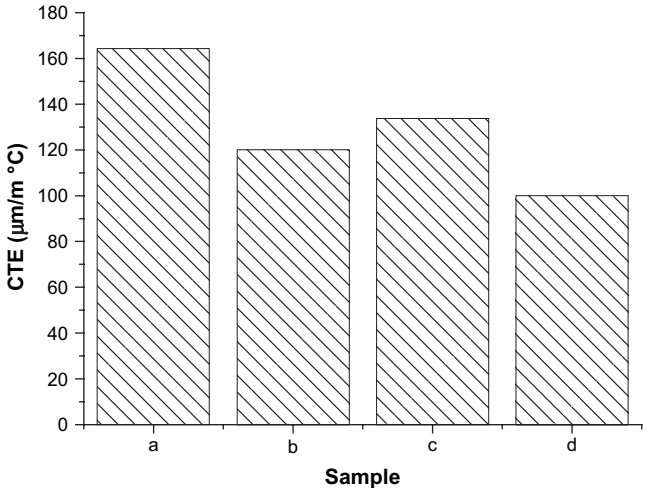

Fig. 7. Coefficient of thermal expansion of (a) pure PS, (b) the nanocomposite formed with C_{20}, (c) the nanocomposite formed with C_{20}–4VB, and (d) the nanocomposite formed with C_{20}–POSS.

sharp. Polymer/clay nanocomposites provide improvements both on thermal and dimensional stabilities. As shown in Fig. 7 and Table 1, the CTE of the virgin PS is 164 μm/m °C while the CTEs for C_{20}/clay/PS, C_{20}–4VB/clay/PS, and C_{20}–POSS/clay/PS are 120, 134, and 100 μm/m °C, respectively. The maximum reduction in coefficient of thermal expansion is from C_{20}–POSS/clay/PS, 39% lower than the virgin PS.

The obtained lower CTE from these composites can be attributed to the particle rigidity and fine dispersion of the clay platelets in the PS matrix. The incorporation of the modified clay can reduce CTE and provides products with good dimensional stability.

4. Conclusions

In this paper, we have employed the novelty of the preparation of the C_{20}–POSS and C_{20}–4VB containing intercalated agents. Syntheses of exfoliated nanocomposites via emulsion polymerization of styrene in the presence of 3 wt% clay containing the C_{20}, C_{20}–4VB, and C_{20}–POSS intercalated agents were prepared, respectively. XRD results show that *d* spacing increases from 1.28 nm to 3.95, 3.33, and 3.80 nm after intercalation. The C_{20}–4VB containing vinylbenzyl group results in more effective in promoting fully exfoliated structure in polystyrene matrix. All modified clay nanocomposites result in higher T_g and higher thermal degradation temperature than the virgin PS, especially for the C_{20}–POSS/clay nanocomposite resulting in 25 °C increase in the thermal degradation temperature. These well distributed clay platelets tend to retard the segmental movement of PS and result in reduced CTE. The incorporation of the 3 wt% clay leads to improvements in thermal stability, slight increase in glass transition temperature, and decrease in coefficient of thermal expansion.

Acknowledgments

The authors thank the National Science Council, Taiwan, for financially supporting this research under Contract NSC-95-2221-E-009-118 and NSC-96-2120-M-009-009.

References

[1] Vaia RA, Ishii H, Giannelis EP. Chem Mater 1993;5:1694.
[2] Chen G, Liu S, Chen S, Qi Z. Macromol Chem Phys 2001;202:1189.
[3] Chen G, Liu S, Zhang S, Qi Z. Macromol Rapid Commun 2000;21:746.
[4] Chen G, Ma Y, Qi Z. J Appl Polym Sci 2000;77:2201.
[5] Chen G, Qi Z. J Mater Res 2000;15:351.
[6] Kurian M, Dasgupta A, Galvin ME, Ziegler CR, Beyer FL. Macromolecules 2006;39:1864.
[7] Gilman JW. Appl Clay Sci 1999;15:31.
[8] Ogata N, Kawakage S, Ogihara T. Polymer 1997;38:5115.
[9] Langat J, Bellayer S, Hudrlik P, Hudrlik A, Maupin PH, Gilman JW, et al. Polymer 2006;47:6698.
[10] Fina A, Tabuani D, Frache A, Camino G. Polymer 2005;47:7855.
[11] Kawasumi M, Hasegawa N, Kato M, Usuki A, Okada A. Macromolecules 1997;30:6333.
[12] Hasegawa N, Okamoto H, Kawasumi M, Usuki A. J Appl Polym Sci 1999;74:3359.
[13] Fu X, Qutubuddin S. Polymer 2001;42:807.
[14] Lan T, Kaviratna PD, Pinnavaia TJ. J Phys Chem Solids 1996;57:1005.
[15] Lan T, Pinnavaia TJ. Chem Mater 1994;6:2216.
[16] Biswas M, Ray SS. Adv Polym Sci 2001;155:167.
[17] Vaia RA, Jandt KD, Karamer EJ, Giannelis EP. Macromolecules 1995;28:8080.
[18] Usuki A, Kojima Y, Kawasumi M, Fukushima Y, Okada A, Fukushima Y, et al. J Mater Res 1993;8:1179.
[19] Kojima Y, Usuki A, Kawasumi M, Okada A, Fukushima Y, Kurauchi T, et al. J Mater Res 1993;8:1185.
[20] Yano K, Usuki A, Okada A, Kurauchi T, Kamigaito O. J Polym Sci Part A Polym Chem 1993;31:2493.
[21] Wang MS, Pinnavaia TJ. Chem Mater 1994;6:468.
[22] Messersmith PB, Giannelis EP. J Polym Sci Part A Polym Chem 1995;33:1047.
[23] Usuki A, Kato M, Okada A, Kurauchi T. J Appl Polym Sci 1997;63:137.
[24] Kato M, Usuki A, Okada A. J Appl Polym Sci 1997;66:1781.
[25] Hasegawa N, Kawasumi M, Kato M, Usuki A, Okada A. J Appl Polym Sci 1998;67:87.
[26] Moet A. Mater Lett 1993;18:97.
[27] Ray SS, Okamoto M. Prog Polym Sci 2003;28:1539.
[28] Usuki A, Hasegawa N, Kato M. Adv Polym Sci 2005;135:179.
[29] Song XY, Geng HP, Li QF. Polymer 2006;47:3049.
[30] Liu Y, Zheng S, Nie K. Polymer 2005;46:12016.
[31] Huang X, Brittain WJ. Macromolecules 2001;34:3255.
[32] Beyer FL, Beck Tan NC, Dasgupta A, Galvin ME. Chem Mater 2002;14:2983.
[33] Vaia RA, Vasudevin S, Krawiec W, Scanlon LG, Giannelis EP. Adv Mater 1995;7:154.
[34] Giannelis EP. Adv Mater 1996;8:29.
[35] Gilman JW, Morgan AB, Harris RH, Trulove PC, Delong HC, Sutto TE. Polym Mater Sci Eng 2000;83:59.